JoT JOURNAL OF TURBULENCE

http://jot.iop.org/

Prediction of turbulent transition in boundary layers using the turbulent potential model

Chang Wang and Blair Perot

Department of Mechanical and Industrial Engineering, University of Massachusetts, Amherst, MA 01003, USA
E-mail: changw@acad.umass.edu

Received 29 January 2002
Published

Abstract. A turbulent potential model is applied to predict the transition in boundary flows. Without assuming any constitutive relation between the turbulence and mean flow variables, this model has the ability to accurately predict strong non-equilibrium flows, but the computation cost for this is only comparable to two equation models and so is the model complexity. Model predictions for a number of transitional flows are presented, which include: bypass transition and natural transition flat plate occurring in Blasius boundary flows with a series of free-stream turbulence intensities, effects of pressure gradients, relaminarization in channel flow and the sensitivity of natural transition to acoustic level. The results are compared to experimental data and other model predictions whenever possible.

PACS numbers: 47.27.Cn, 47.27.Eq

Contents

1 Introduction **2**

2 Motivation **2**

3 Model equations **5**

4 Computation results and discussion **6**
4.1 Flat plate boundary layer in zero pressure gradient 6
4.2 Flat plate boundary layer in non-zero pressure gradient 8
4.3 Acoustic effects on natural transition 10
4.4 Relaminarization in turbulent channel flow 12

5 Conclusion **14**

 PII: S1468-5248(02)35220-2 1468-5248/02/000001+15$30.00

JoT 3 (2002) 001

1. Introduction

Predicting the onset of turbulent flow is a critical component of many engineering and environmental flows. The characteristics of laminar and turbulent boundary layers are so different that the precise location of this relatively abrupt transition can have a profound influence on the overall drag, heat transfer, and performance properties of devices that operate in the transitional regime. The prediction of boundary layer transition is complicated by the fact that it does not correspond very directly to the onset of instability. Stability analysis for boundary layers is well developed and very predictive of the behaviour of small disturbances. However, the instabilities go through a series of complex nonlinear and three-dimensional processes before turbulence itself actually develops. In addition, stability analysis is less helpful with the prediction of bypass transition where external free-stream disturbances bypass the classic instability mechanisms and initiate the nonlinear three-dimensional transition process directly.

Traditional methods for predicting transition rely on correlations. For example, [20] suggest the implicit correlation $1690Re_{x,tr}^{-1/2} = 0.312(m+0.11)^{-0.528} + 4.8\delta_{99}^2 Re_{x,tr}^{1/2} T^2$ where $Re_{x,tr}$ is the transition Reynolds number based on the local free-stream velocity U, the parameter m is related to the dimensionless pressure gradient ($m = 0$ for zero pressure gradient), δ_{99} is the local 99% boundary layer thickness, and $T = \sqrt{(2/3)k}/U$ is the local free-stream turbulence intensity. This is only one of many proposed correlations. While they appear relatively simple, they are actually quite awkward to implement in a general purpose CFD code. In a general code, correlations require each point on the boundary to determine non-local quantities, such as free-stream values, distance downstream from the leading edge and boundary layer thickness. Unambiguous definitions for such quantities in a general situation are very difficult to formulate. Many CFD codes simply resort to requiring the user to specify the transition location. Once the transition location has been determined, there is the further difficulty of determining how the turbulence model should be prompted to become active. Solutions to this problem range from specifying large turbulent kinetic energy at the wall where transition is expected to occur to specifying local large source terms in the turbulence evolution equations (artificial production). None of these methods of 'tripping' the turbulence model are particularly reflective of the actual physical transition process, and add further ambiguity to the already uncertain transition location. In addition, 'tripping' of this sort is largely code dependent, so that the same theoretical model can produce different results in different codes, or even within the same code using different meshes.

An alternative approach is to use the turbulence model itself to predict the transition location. This is a very natural approach in bypass transition, since the model is effectively *on* in the free stream anyway to predict the free-stream turbulence. A number of studies of boundary layer bypass transition prediction using low Reynolds number k–ε models have been performed, and [13] gave good reviews of how various flavours of the k–ε models perform. The overall conclusion is that none performs well for all the flows considered. More recent work using a k–ε intermittency model (Suzen and Huang 2001) has shown more success. However, none of these models attempts to predict natural transition or relaminarization.

2. Motivation

While the idea of using Reynolds averaged Navier–Stokes (RANS) models to predict transition may have originally been motivated by practical considerations such as ease of implementation, it also has a solid theoretical justification that has not been discussed previously. The derivation of the RANS and accompanying Reynolds stress transport (RST) equations are simply a

mathematical reformulation of the governing Navier–Stokes equations. There are no physical assumptions or restrictions on the range of applicability of these equations, as presented below.

$$\frac{\partial \boldsymbol{u}}{\partial t} + \nabla \cdot (\boldsymbol{u}\boldsymbol{u}) = -\nabla p + \nabla \cdot \nu \nabla \boldsymbol{u} - \nabla \cdot \boldsymbol{R} \tag{1a}$$

$$\nabla \cdot \boldsymbol{u} = 0 \tag{1b}$$

$$\frac{\partial \boldsymbol{R}}{\partial t} + \boldsymbol{u} \cdot \nabla \boldsymbol{R} = \nu \nabla^2 \boldsymbol{R} - \left(\overline{u_i' u_k'} \frac{\partial \bar{u}_j}{\partial x_k} + \overline{u_j' u_k'} \frac{\partial \bar{u}_i}{\partial x_k} \right) + \overline{\frac{p'}{\rho} \left(\frac{\partial u_i'}{\partial x_j} + \frac{\partial u_j'}{\partial x_i} \right)} - 2\nu \overline{\frac{\partial u_i'}{\partial x_k} \frac{\partial u_j'}{\partial x_k}} - \frac{\partial}{\partial x_k} \left(\overline{u_i' u_j' u_k'} + \overline{\frac{p' u_i'}{\rho}} \delta_{jk} + \overline{\frac{p' u_j'}{\rho}} \delta_{ki} \right) \tag{2}$$

where $\boldsymbol{u}$ is the mean velocity, and $\boldsymbol{R}$ is the single point, second-order correlation of the fluctuating velocity. The derivation of these equations can be found in numerous textbooks. The first term in parentheses is the production term. This term does not require a model if equation (2) is solved. The subsequent terms are pressure strain, dissipation, turbulence transport and pressure transport terms, all of which require a model.

This rearrangement of the equations is undertaken in order to isolate what is computable (the mean flow), from the underlying (incomputable) turbulent velocity fluctuations. The price that is paid for isolating this computable system from the governing (and essentially intractable) Navier–Stokes equations is that the equations are unclosed, and models must be constructed to represent the effect of the turbulence fluctuations on the mean flow. It is these models, not the equations themselves, that may, or may not, be able to capture the nonlinear transition to turbulence. The RST equation (2) is the basis for many turbulence models (including k/ε, algebraic Reynolds stress, and turbulent potential models) and is the starting point for this discussion.

In a fully turbulent flow all the unclosed terms in the RST equations require modelling, none can be neglected. However, in a transitioning flow, the fluctuations are relatively small and one might expect the turbulent transport term, which involves a velocity triple product, to be very small. Linear stability analysis is akin to assuming that the turbulent transport term is identically zero. Furthermore, this term can only redistribute energy spatially. It does not cause any increase in overall turbulence levels—the hallmark of a transitioning flow. The pressure-transport term (last term in equation (2)) is small in fully developed turbulent boundary layers, and also can only redistribute energy, so we will assume that like the turbulent transport term it is not a critical process in transition. The dissipation term (involving viscosity) is also expected to be small when the transition process initiates. Eventually, we know that the turbulence will create very strong local gradients so that the dissipation term will balance the other terms in the RST equation. However, early in the transition process, the gradients will be relatively weak and the turbulence will grow very rapidly, indicating dissipation is not dominant. The dissipation model is expected to have a significant influence on the exact nature of the overshoot (in turbulence intensities and skin friction) that occurs at the end of transition just before fully developed turbulence is obtained, but it is unlikely to have much effect on the much more critical transition location.

The final modelled term, the pressure–strain correlation cannot be neglected in the transition process. The equation for the fluctuating pressure

$$p'_{,ii} = -2u_{j,i}u'_{i,j} + R_{ij,ij} - (u'_i u'_j)_{,ij} \tag{3}$$

shows that the pressure has two components, one of which is dependent on the mean shear, and is linearly proportional to the fluctuating velocity. This rapid pressure–strain term is of the same order of magnitude as the production term, and tends to reduce some, but not all, of the

production. Rapid distortion theory (RDT) can tell us a great deal about how this term should behave in certain limits. The RDT analysis is formally restricted to spatially homogeneous fluctuations but is otherwise well suited to the problem of transition.

In summary, turbulence models that accurately capture production and rapid pressure–strain processes are expected to have a good chance of predicting turbulent transition. Models for the pressure transport, turbulent transport, and dissipation are only expected to influence the very last stages of transition (the overshoot recovery) and should have little effect on the critical transition location. Most models for the rapid pressure strain usually only capture rapid shear correctly because this is the important case for boundary layer and free-shear flows. Reference [12] have a modelling framework that can capture any rapidly distorting flow.

Due to the complexity of solving the RST equations, two-equation models such as k/ε are very popular. The k-equation is derived by taking one half of the trace of equation (2):

$$\frac{\partial K}{\partial t} + \boldsymbol{u}\cdot\nabla K = -\frac{1}{2}\overline{u_j' u_k'}\frac{\partial u_j}{\partial x_k} - \frac{\partial}{\partial x_k}\left\{\overline{u_j'\left(\frac{1}{2}u_i' u_i' + \frac{p'}{\rho}\right)}\right\} - \nu\overline{\left(\frac{\partial u_i'}{\partial x_j}\right)^2} + \nu\nabla^2 K. \tag{4}$$

Two very important changes take place when only the k-equation is solved. Firstly, pressure strain disappears entirely. This is because this term only redistributes energy between various Reynolds stress components, it does not influence the overall energy content. Unlike spatial redistribution (transport terms) this intercomponent redistribution *is* important, particularly in the boundary layer. It takes energy out of the amplified streamwise fluctuations and transfers it to the normal and spanwise fluctuations, damping the streamwise fluctuation growth and feeding the normal and spanwise velocity fluctuations. Two-equation models are fundamentally incapable of capturing physical processes that involve intercomponent energy redistribution. In addition, the production term is no longer exact. The Reynolds stress tensor in this term must now be modelled. The classic Boussinesq eddy viscosity model is

$$\boldsymbol{R} = \tfrac{2}{3}K\boldsymbol{I} - \nu_T(\nabla\boldsymbol{u} + \nabla\boldsymbol{u}^T) \tag{5}$$

where the eddy viscosity is given by $\nu_T = C_\mu K^2/\varepsilon$. More complicated versions of this equation are possible and are referred to as nonlinear eddy viscosity models or algebraic Reynolds stress models. They all have the same fundamental problem for predicting transition. These models assume that the fluctuations are somehow in equilibrium with the mean flow. They suppose that a given shear level results in a given turbulence level. The transition process is as far from an equilibrium situation as possible. During transition, fluctuation amplitudes grow exponentially in time (moving with the fluid), while shear levels remain almost constant.

Despite these difficulties, it is interesting to note that two-equation models still can produce qualitatively transition-like behaviour, with a rapid increase in turbulence levels and skin friction from low initial levels. This suggests that these differential equations, and by inference the modelled RST equations, have the mathematical capability to produce exponentially growing solutions, and transitional behaviour. With the added accuracy in the production and rapid pressure–strain terms, it is expected that RST models could potentially constitute a very accurate transition prediction methodology. However, classic RST models represent a significant investment in programming complexity and computational resources. The turbulent potential model used in this work [9, 11, 21] represents an effective compromise. It is a reformulation of the RST equations that retains the non-equilibrium and energy redistribution physics, but which can be implemented at a computational cost and programming complexity comparable to the very popular two-equation models. The turbulent potential model's formulation and success in predicting fully turbulent flows has been discussed in prior publications [2, 10, 16]. In this paper, we focus on its unique abilities to predict transition in boundary layer flows. We demonstrate the ability to predict bypass transition, the effects of pressure gradients, natural transition, relaminarization, and the effect of noise levels on natural transition.

3. Model equations

The turbulent potential model used in this work is a slight modification of the model proposed by [9]. The basic motivation and derivation remains the same.

$$\frac{Dk}{Dt} = \nabla \cdot (\upsilon + \upsilon_t \bar{\sigma}_k)\nabla k + P - \varepsilon \tag{6a}$$

$$\frac{D\varepsilon}{Dt} = \nabla \cdot (\upsilon + \upsilon_t \bar{\sigma}_\varepsilon)\nabla \varepsilon + \frac{\hat{\varepsilon}}{k}(C_{\varepsilon 1}P - C_{\varepsilon 2}\varepsilon) \tag{6b}$$

$$\frac{D\phi}{Dt} = \nabla \cdot (\upsilon + \upsilon_t \bar{\sigma}_\phi)\nabla \phi + \prod_{\phi}^{slow} + \prod_{\phi}^{rapid} - \varepsilon_\phi + C_t\left(1 - 1.5\frac{\phi}{k}\right)P\left(\frac{\upsilon_t}{\upsilon}\right)^{1/2} \tag{6c}$$

$$\frac{D\psi}{Dt} = \nabla \cdot (\upsilon + \upsilon_t)\nabla \psi + \prod_{\psi}^{slow} + \prod_{\psi}^{rapid} - \varepsilon_\psi + C_t\left(\frac{\upsilon_t}{\upsilon}\right)^{1/2}\omega k. \tag{6d}$$

Constants and parameters are given by:

$$P = \psi \cdot \omega, \quad \upsilon_t = C_\mu \frac{\phi k}{\hat{\varepsilon}}, \quad \alpha = \frac{1}{1 + 1.5\frac{\phi}{k}}$$

$$\hat{\varepsilon} = \varepsilon/[1 + 10\nu|\nabla k^{1/2}|/k]$$

$$C_\mu = 0.21, \quad C_{p1} = 2.0\frac{\upsilon_t}{\upsilon_t + 5\upsilon}, \quad C_{p2} = \frac{3}{5}, \quad C_{p4} = \frac{6}{7}, \quad C_t = 0.0033$$

$$\sigma_k = 0.33 + 0.67P/\hat{\varepsilon}$$

$$\sigma_\varepsilon = 0.33 + 0.5P/\hat{\varepsilon}$$

$$\sigma_\phi = 0.33$$

$$C_{e1} = 1.45, \quad C_{e2} = 1.83 - 0.16\exp\left(-0.25\frac{k^2}{\upsilon\varepsilon}\right).$$

The slow pressure–strain models are

$$\prod_{\phi}^{slow} = -(\upsilon + \upsilon_t\bar{\sigma}_\phi)\nabla\left(\frac{\phi}{k}\right)\nabla k + C_{p1}\frac{\hat{\varepsilon}}{k}(2\alpha - 1)\phi + \ (C_{p2} + C_{p4})\left[\frac{(\psi/k)(\psi/k)}{\upsilon_t/k(1 + 25/Re)} - P/k\right]\phi$$

and

$$\prod_{\psi}^{slow} = -2(\upsilon + \upsilon_t)\nabla\left(\frac{\psi}{k}\right)\nabla k - C_{p1}\frac{\hat{\varepsilon}}{k}(1 - \alpha)\psi.$$

The fast pressure–strain models are

$$\prod_{\phi}^{rapid} = C_{p2}\frac{P}{k}\phi$$

and

$$\prod_{\psi}^{rapid} = (1 - C_{p2})\phi\omega + C_{p2}\psi\frac{P}{k} + C_\mu(2\alpha - 1)\psi\omega - 2\alpha\frac{P}{k}\psi.$$

The dissipation terms are given by

$$\varepsilon_\phi = 2(\upsilon + \upsilon_t\bar{\sigma}_\phi)\nabla\phi^{1/2} \cdot \nabla\phi^{1/2} + 2\alpha\frac{\phi}{k}\varepsilon$$

and

$$\varepsilon_\psi = \alpha \frac{\psi}{k} \varepsilon.$$

Transport terms are modelled by the υ_t in the diffusion term. The two terms involving C_t in the turbulent potential equations (6c) and (6d) are the critical terms for transition. Interestingly, because C_t is so small, these terms have no influence on fully developed turbulent flows. The model shows no perceptible difference in its predictions when C_t is set to zero in fully turbulent flows. However, it has a very direct effect on transition, with higher values of C_t causing transition to occur earlier. We have used a value of 0.0033 in all the results presented in the paper, but it should be observed that the model has the unique ability to explicitly control transition if the user so desires.

The k–ε equations are a fairly standard implementation with slightly modified definitions of some of the constants. Standard definitions for these constants will also work quite adequately, these are just our own preferences. What is important to emphasize is that although we are solving k–ε transport equations this model is nothing like a k/ε model. In this model the potentials are defined by the exact relationship $\nabla \cdot R = \nabla\phi + \nabla \times \boldsymbol{\psi}$, so k and ε are *only* used to model the source terms in the turbulent potential evolution equations. They are not used to directly calculate the Reynolds stress tensor, or the effect of the turbulence on the mean flow.

4. Computation results and discussion

A number of different transitional flows have been calculated using the present model, and are compared to experimental data. The results presented below include: transition in flat plate Blasius boundary layers with different levels of free-stream turbulence intensity, including very low level leading to natural transition, the effects of variable pressure gradients and noise on flat plate transition, and relaminarization in turbulent channel flow.

4.1. Flat plate boundary layer in zero pressure gradient

The process of transition is studied by looking at the evolution of the friction coefficient along the streamwise direction. The friction coefficient is a very sensitive indicator of transition that increases dramatically as transition occurs. The model predictions are compared to experimental data with different turbulence intensities. The mean velocity is initially uniform flow for all cases and the initial values of velocity U_0, turbulence Reynolds number $Re_T = k^2/(\nu\varepsilon)$, turbulence intensity level $Tu = (2/3k)^{1/2}/U_\infty$ for five experimental cases with different turbulence intensities are given in table 1. The initial values of the turbulent kinetic energy k are determined using $k = 3/2(Tu \cdot U_0)^2$. For the $Tu = 0.03$, 1.25 and 1.3% cases, the initial turbulent dissipation rate ε is calculated from Re_T using $\varepsilon = k^2/(\nu Re_T)$ and the value of Re_T is assumed. The results are not very sensitive to reasonable values of Re_T. For the $Tu = 3\%$ (T3A) and $Tu = 6\%$ (T3B) cases, the data for k are available, and the initial values of ε are determined from $\varepsilon = -U_\infty \frac{\mathrm{d}k_\infty}{\mathrm{d}x}$, where the subscript '$\infty$' represents parameters in the free stream. The values of Re_T for these two cases listed in table 1 are just calculated from ε. The initial potentials ϕ and ψ are set as $2/3k$ and zero respectively. All experiments were performed in air so $\nu = 1.55 \times 10^{-5}$ was used in every case.

The friction coefficient is plotted against, Re_x, the Reynolds number based on downstream position, in figure 1. The friction coefficient correlations for laminar and turbulence flows, $C_f = 0.664 Re_x^{-1/2}$ and $0.027 Re_x^{-1/7}$ respectively, are also plotted with dashed curves for comparison. Overall, the ability of the present model to predict the critical transition location is quite good. However, the natural transition case, $Tu = 0.03\%$, shows some discrepancy with the

Table 1. Initial flow parameters at the leading edge of a zero pressure gradient boundary layer.

U_0 (m s^{-1})	Re_T	Tu (%)	Source
24.4	100	0.03	[14]
22	250	1.25	[1]
14.42	250	1.3	[5]
5.4	200	3.0	ERCOFTAC, T3A
9.4	200	6.0	ERCOFTAC, T3B

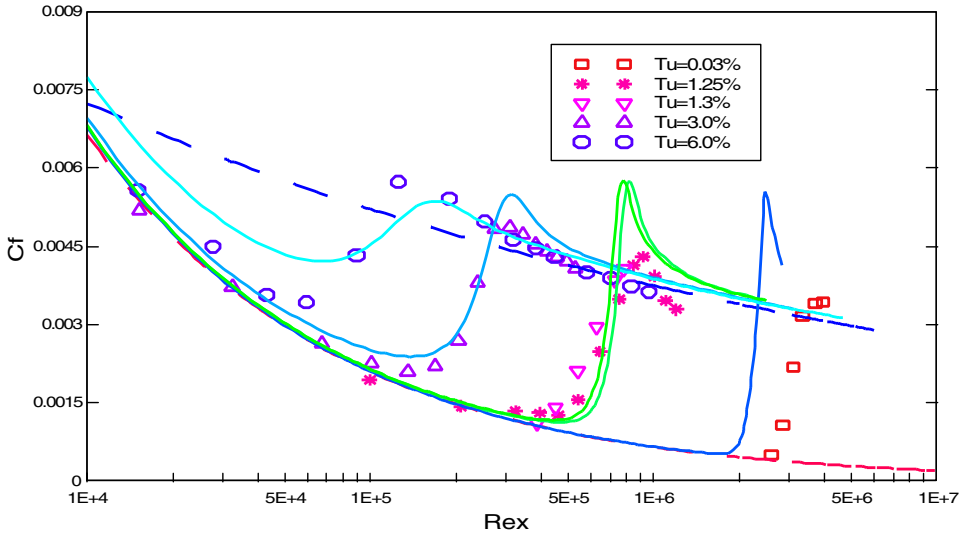

Figure 1. Transition in zero pressure gradient boundary layer at various initial turbulence intensities. The symbols represent experiment data and the curves are the present results. The dashed curves are fully laminar and fully turbulent correlations.

experimental data of [14] at 2.8×10^6. Actually, this discrepancy is somewhat expected given the model initial conditions. Experiments of natural transition show a wide range of transition locations from a high value of $Re_x = 5.0 \times 10^6$ measured by [18] to classical predictive theories, such as the e^9 rule, which predict a value of 2.0×10^6 [17]. This range of results is commonly attributed to different noise levels in the various experiments. We show later that the model can actually predict the entire range of natural transition experiments by varying the model initial conditions. We believe that the ability of this model to predict natural transition is a unique characteristic that is not demonstrated by other RANS models.

The other significant departure of the model predictions from the experiments is in the overshoot of the friction coefficient that occurs at the very end of the transition process and in the transition length. Predicting this overshoot and length correctly is not as important as predicting the transition location itself. Interestingly, the model does show the characteristic overshoot behaviour found in experiments, but over predicts the extent of this overshoot. Our current hypothesis is that this discrepancy is largely caused by the use of boundary layer equations to solve the velocity and turbulence variables, and is not due to the model itself. The boundary layer equations are based on the premise that streamwise second derivatives are small. During the later part of transition, as the flow suddenly becomes turbulent, the boundary layer

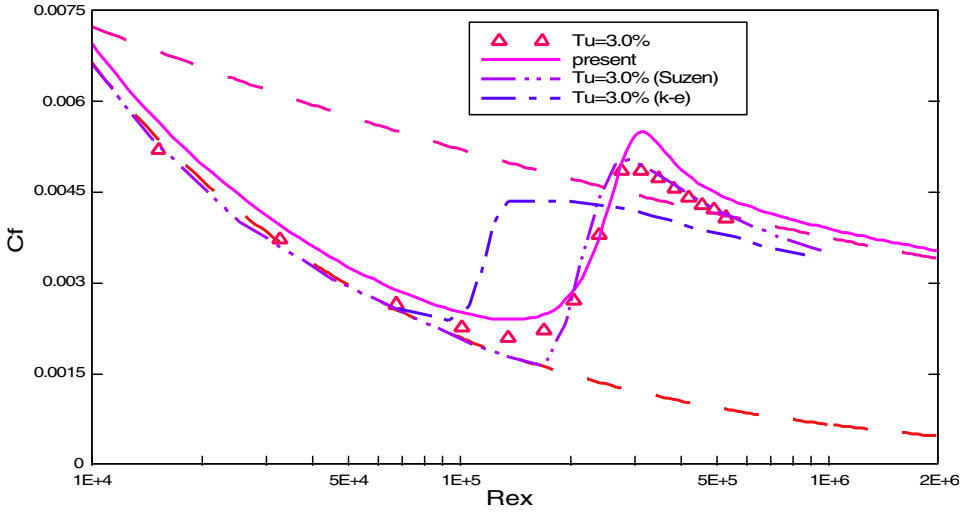

Figure 2. Comparison of predictions of transition in zero pressure gradient boundary layer for T3A case. the symbols represent experimental data and the curves are the predictions.

grows quite dramatically, and the assumption of small streamwise second derivatives is not very accurate. Including these streamwise derivatives is expected to add considerable diffusion and to significantly reduce the current excessive overshoot behaviour. The fact that the overshoot error increases as the turbulence intensity decreases is consistent with this behaviour, because the lower intensity transition events are also more abrupt and therefore violate the boundary layer approximations the most severely.

Two other numerical predictions, both performed by [15], but using their k–ε intermittency model and another k–ε model [6] respectively, are plotted in figure 2 for the T3A case. The k–ε model predictions are not particularly good for this particular case. In contrast, the model of Suzen and Huang captured the late stage of the transition region (including the overshoot) very well, but the transition onset was delayed. The present calculation, as shown in figure 2, shows a smoother transition behaviour. In other words, the present model predicts not only a correct position of transition onset, but also a fairly accurate length of the transition region.

The comparison of the Reynolds number based on momentum thickness, Re_θ, and shape factor, H, with experiments and results from other numerical models are shown in figures 3 and 4 respectively for the T3A case. It can be noted that the present prediction always remains between the other two simulations. The fact that the model of Suzen and Huang has a slight later prediction of the onset of transition is also visible from the H curves.

The streamwise mean velocity profiles calculated using the present model are compared at four downstream stations with the experimental T3A data and the predictions of Suzen and Huang in figures 5(a)–(d). It is evident from these figures that the model predictions agree very well with the experimental data even for the detailed mean velocity profiles.

4.2. Flat plate boundary layer in non-zero pressure gradient

Model predictions of transition in two variable pressure gradient boundary layers are compared with the experimental data of [3] in figure 6. The initial turbulence levels of these two cases are 3.0% (T3C3) and 6.6% (T3C1) respectively. For both these flows, the pressure gradient is initially negative (favourable) and then positive (adverse) in a profile that was designed to roughly approximate the flow over a turbine blade. The pressure gradient profiles for the two

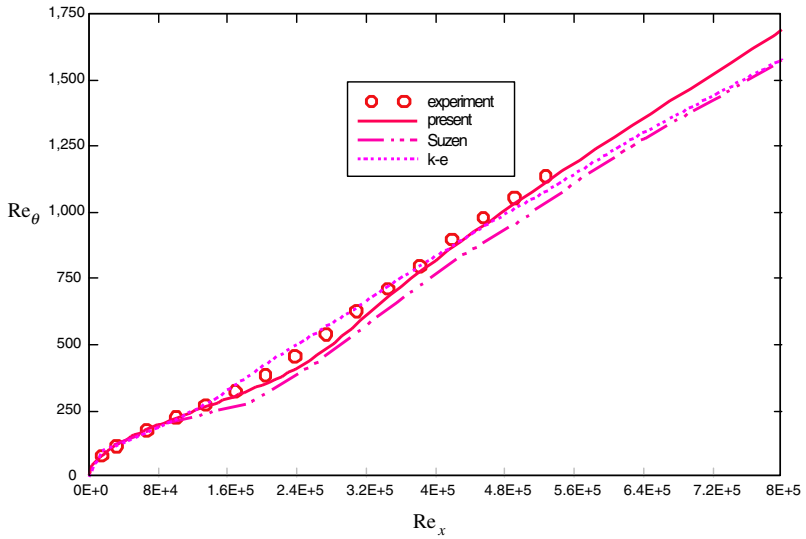

Figure 3. Comparison of Re_θ for T3A case.

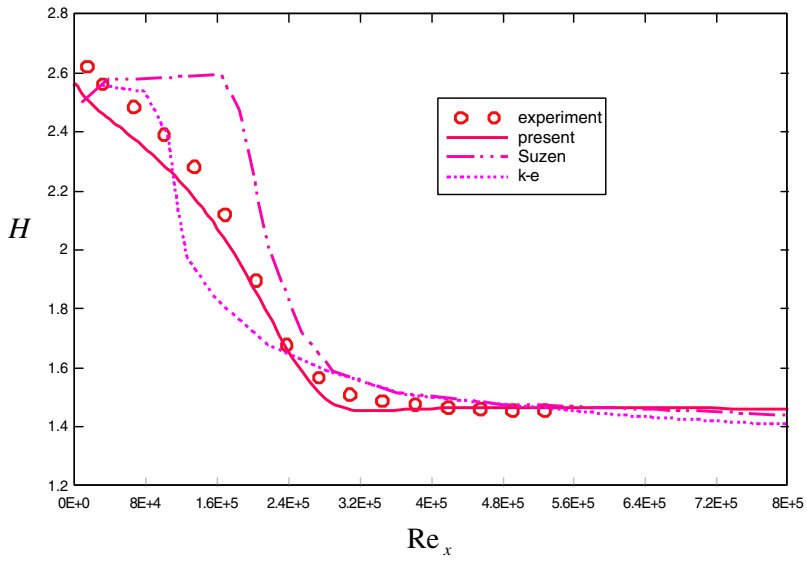

Figure 4. Comparison of H for T3A case.

different cases are roughly equivalent. The initial conditions are listed in table 2 and are fully determined by the initial experimental data. It is very difficult to use correlations to predict this variable pressure gradient flow because the pressure gradient does not correspond closely to any single Falkner–Skan situation. In addition, the RANS models tested by [13] showed some difficulty with these cases.

The model predicts the transition location in these complex variable pressure gradient boundary layers quite well. Note that in both cases the initially favourable pressure gradient has delayed transition compared to the flat plate case. The pressure gradient data are not provided beyond the range of the experimental data, so we cannot continue the 3% case beyond the experimental data. Predictions given by [15] are compared with the present calculation for the T3C1 case again in figure 7.

Figure 8 shows the comparison of Re_θ computed by the present model and the two other

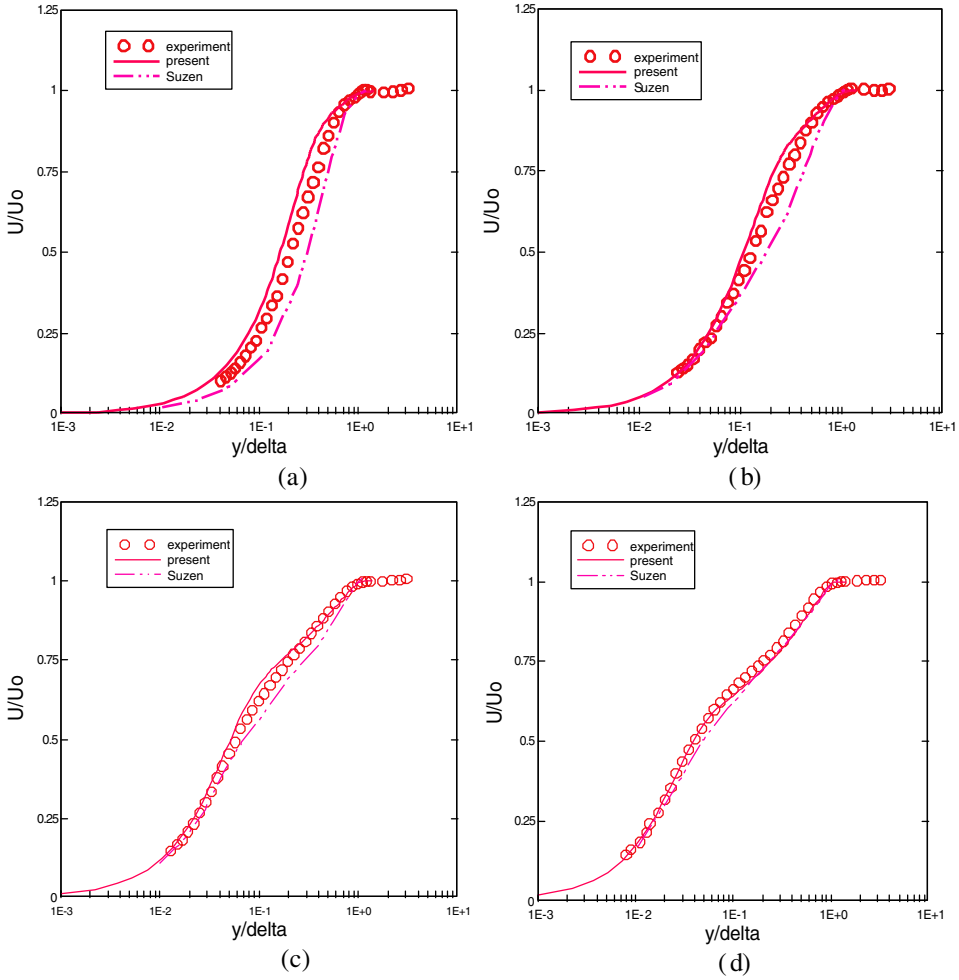

Figure 5. Mean streamwise velocity profiles for T3A case: (a) $Re_x = 1.35 \times 10^5$; (b) $Re_x = 2.04 \times 10^5$; (c) $Re_x = 2.74 \times 10^5$; (d) $Re_x = 4.19 \times 10^5$.

Table 2. Initial flow parameters at the leading edge of a variable pressure gradient flat plate boundary layer.

U_0 (m s^{-1})	Re_T	Tu (%)	Source
5.9	160	6.6	ERCOFTAC, T3C1
3.7	100	3.0	ERCOFTAC, T3C3

models with the experimental data for the T3C1 case. Predictions of the shape factor profiles using the three models are plotted in figure 9 along with the experimental data. Again the present model exhibits excellent performance in calculating the shape factor in the transition region.

4.3. Acoustic effects on natural transition

It was mentioned previously that acoustic effects (wind tunnel noise) can have a fairly strong influence on natural transition. The experiment of [18] is commonly assumed to be largely free of acoustic noise, and therefore gives a high 'quiet' transition location of $Re_{x,tr} = 5.0 \times 10^6$. Our

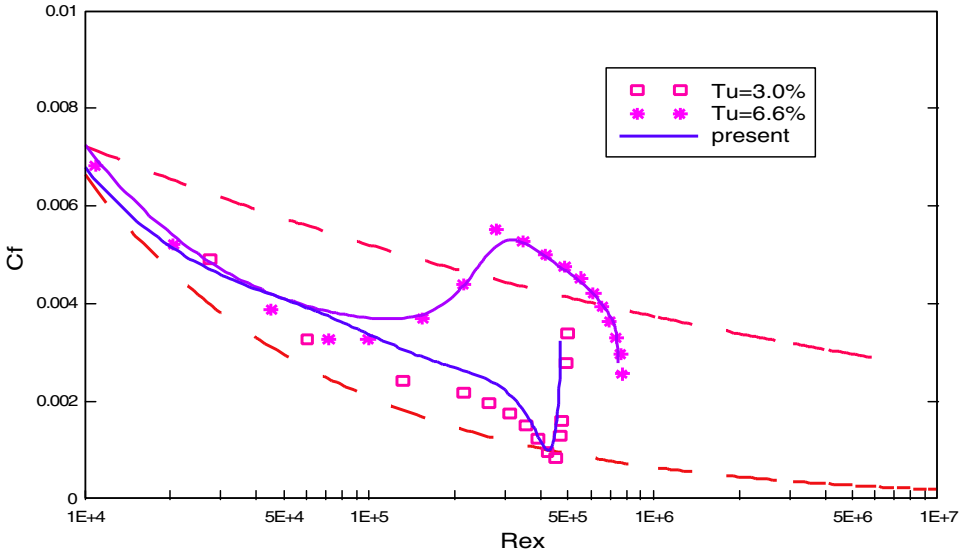

Figure 6. Transition in non-zero pressure gradient boundary layer at various initial turbulence intensities. The symbols represent experimental data and the curves are the present results.

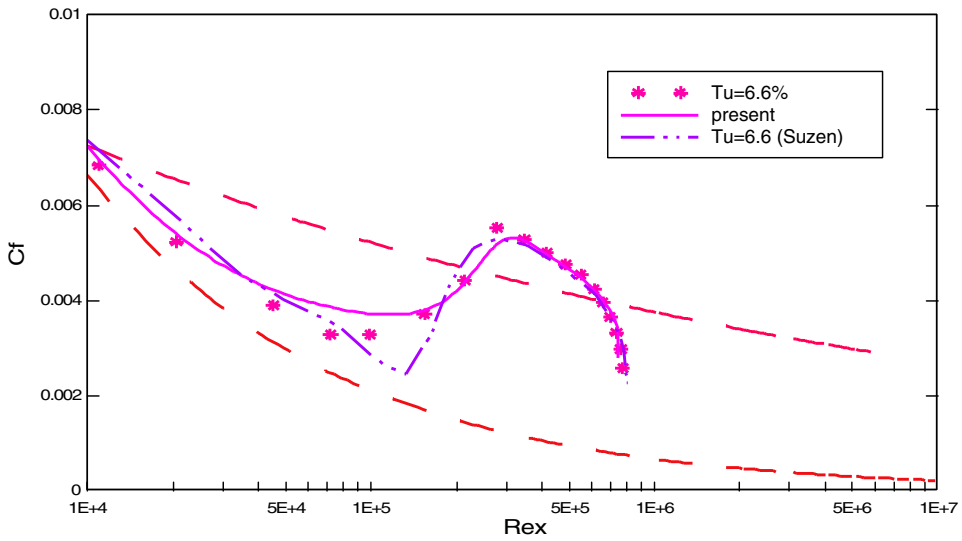

Figure 7. Comparison of predictions of transition in non-zero pressure gradient boundary layer for T3C1 case. The symbols represent experimental data and the curves are the predictions.

initial prediction of $Re_{x,tr} = 2.0 \times 10^6$ is close to the low (noisy) end of the experimental range. The experiments of [14] attempted to reduce noise levels, but were clearly not as successful in this respect as the later experiments of Well.

Interestingly, the turbulent scalar potential represents irrotational fluctuations (see [9]), and could be a very good measure of the average acoustic forcing. Our initial natural transition prediction (figure 1) was with relatively high noise levels of $\phi = 2/3k$, and is actually quite close to 'noisy' experiments. If one reduces the initial scalar potential φ to a value of $0.12k$, the onset of the transition will be delayed to 5.0×10^6, which agrees with [18]. One can also match the

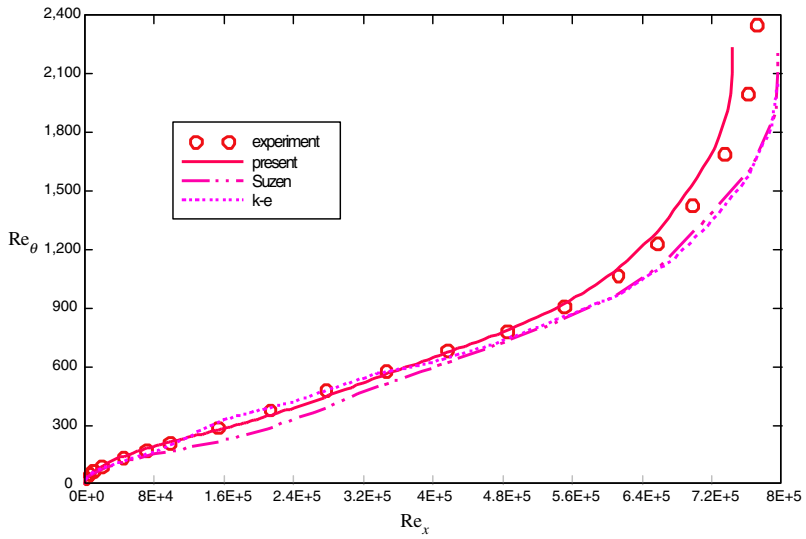

Figure 8. Comparison of Re_θ for T3C1 case.

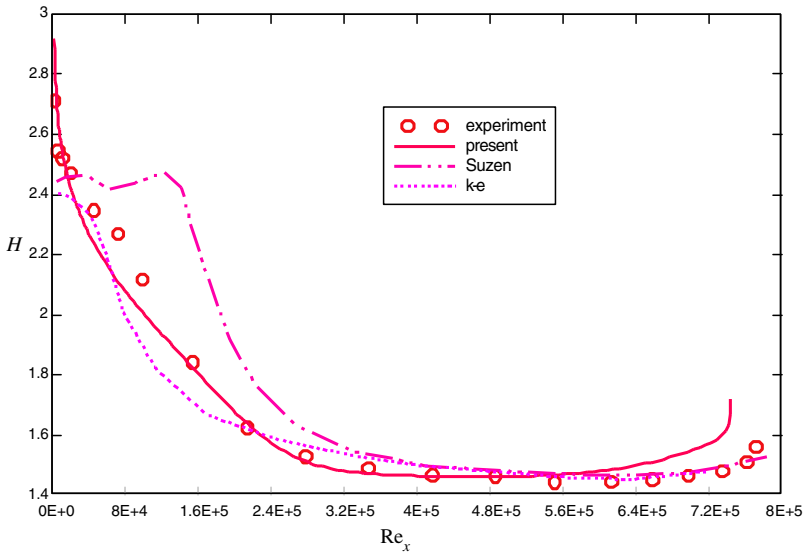

Figure 9. Comparison of H for T3C1 case.

data of [14] $Re_{x,tr} = 2.8 \times 10^6$ in table 1 by using $\phi = 0.4k$. All three simulations are shown in the C_f–Re_x curve plotted in figure 10. This demonstrates the ability of the model to accurately capture the effects of noise on natural transition. The effects of noise on bypass transition are present but are less significant.

4.4. Relaminarization in turbulent channel flow

Almost as critical as transition is the process of relaminarization, where a turbulent flow decays to a laminar state. Relaminarization can occur because of strong stratification, strong rotation, or in the case of channel flow, due to a reduction in the driving pressure gradient. Figure 11 shows predictions of the skin friction in channel flow for various bulk Reynolds numbers $Re = \bar{u}_b h/\upsilon$, where h is the channel half height and $\bar{u}_b$ is the average velocity. The figure also has dashed curves

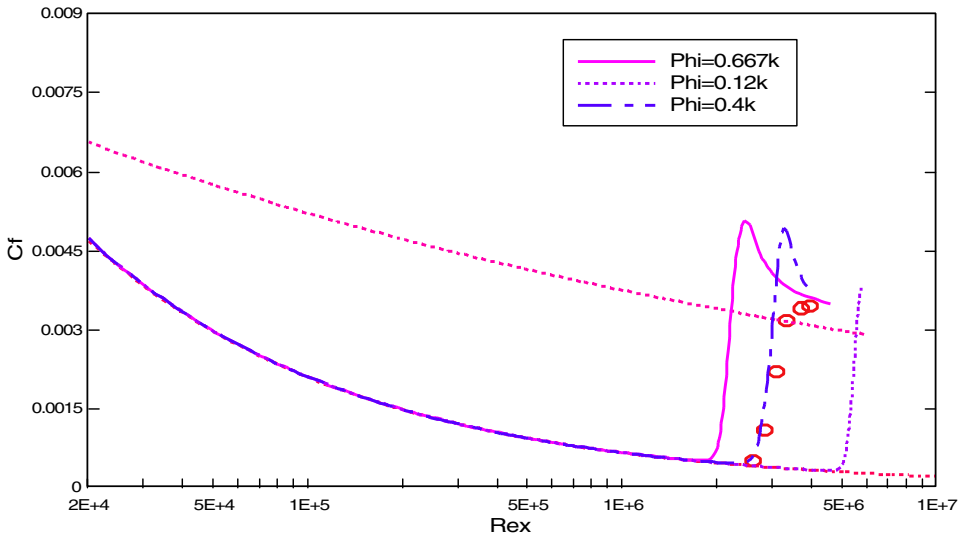

Figure 10. The acoustic effects on the natural transition at $Tu = 0.03\%$. The dashed curves are fully laminar and fully turbulent correlations.

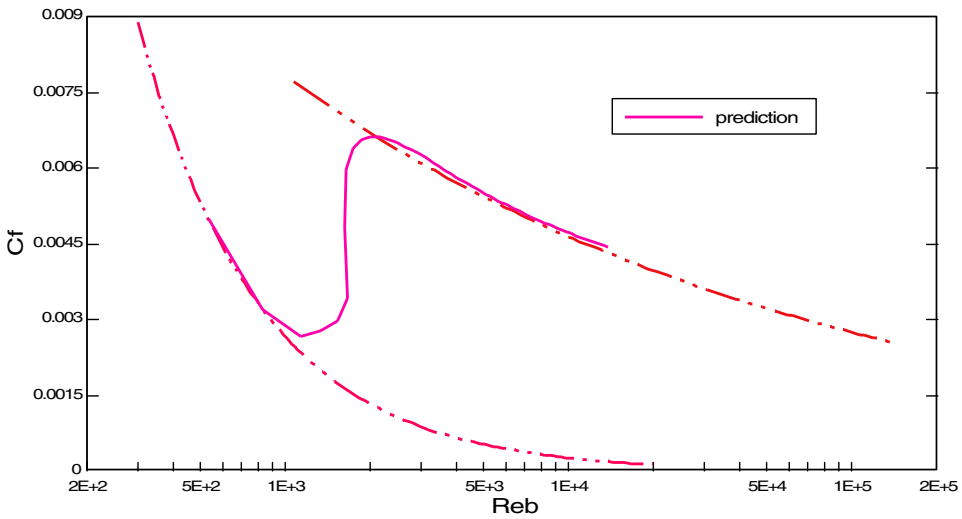

Figure 11. Predictions of the skin friction in channel flow for various bulk Reynolds numbers. The dashed curves are fully laminar and fully turbulent correlations.

for the laminar exact result $C_f = \frac{8}{3}Re^{-1}$ and the turbulent correlation of [4] $C_f = 0.044Re^{-0.227}$. Here the skin friction coefficient is calculated using $C_f = (\tau_w)/(1/2\rho u_0^2)$, where τ_w is the wall shear stress and u_0 is the centre line velocity of the channel. The model shows a clear relaminarization at $Re_b = 1700$ ($Re_\tau = 120$). Experiments and DNS [7] indicate a transition Reynolds number of close to 1000 ($Re_\tau = 60$). So the model could be improved. However, a theoretical study by [8] has shown that the linear instability for a channel flow occurs at $Re_b = 1600$ ($Re_\tau = 110$). It is our observation that this relaminarization location is strongly influenced by the low Reynolds number behaviour of the model (particularly the dissipation and pressure–strain term), and not the transition term itself.

5. Conclusion

The ability of the turbulent potential model to predict transition in a wide variety of boundary layer flows has been demonstrated. This includes the ability to predict everything from natural transition (a first for RANS-based models) to large free-stream turbulence intensities. The model is also demonstrated to be able to accurately calculate the transitional flat plate boundary layer under favourable and adverse pressure gradients. The ability of this model to reflect the effect of noise on the natural transition is also shown by comparison with corresponding experimental data under different conditions. Finally, the relaminarization in turbulent channel flow is successfully captured using this model. The computation cost of the proposed method is comparable to the widely used two-equation models such as k/ε. However, unlike k/ε, the model does not assume equilibrium between the developing instability and/or turbulence fluctuations, and it is this non-equilibrium nature to which we attribute these successful predictions.

Acknowledgments

This work was supported in part by the Air Force Office of Scientific Research and by the Office of Naval Research.

References

[1] Abu-Ghannam B J and Shaw R 1980 Natural transition of boundary layers—the effects of turbulence, pressure gradient, and flow history *J. Mech. Eng. Sci.* **22** 213–28

[2] Are S, Zhang X and Perot J B 2001 Accuracy and conservation properties of a three-dimensional unstructured staggered mesh scheme for fluid dynamics *Int. J. Rotating Machinery* at press

[3] Coupland J 1990a ERCOFTAC Special Interest Group on Laminar to Turbulent Transition and Retransition T3A and T3B Test cases

Coupland J 1990b ERCOFTAC Special Interest Group on Laminar to Turbulent Transition and Retransition T3C Test cases

[4] Dean R B 1978 Reynolds number dependence of skin friction and other bulk flow variables in two-dimensional rectangular duct flow *J. Fluids Eng.* **100** 215–23

[5] Dhawan S and Narasimha R 1958 Some properties of boundary layer flow during the transition from laminar to turbulent motion *J. Fluid Mech.* **3** 418–36

[6] Launder B E and Sharma B I 1974 Application of the energy dissipation model of turbulence to the calculation of flow near a spinning disc *Lett. Heat Mass Transfer* **1** 131–8

[7] Keefe L, Moin P and Kim J 1992 The dimension of attractors underlying periodic turbulent Poiseuille flow *J. Fluid Mech.* **242** 1–29

[8] Orszag S 1971 Accurate solution of the Orr–Sommerfeld stability equation *J. Fluid Mech.* **50** 689–703

[9] Perot J B 1999 Turbulence modeling using body force potentials *Phys. Fluids* **11** 2645–56

[10] Perot J B and Taupier J 2000 Modeling three-dimensional boundary layers using the turbulent potential model *AIAA 2000-0914 (Reno, Nevada, January 2000)*

[11] Perot J B and Wang H 1999 Modeling separation and reattachment using the turbulent potential model *Proc. 4th Int. Conf. on Turbulence Modeling and Measurements (Corsica, France, May 1999)*

[12] Reynolds W C and Kassinos S C 1995 One-point modeling of rapidly deformed homogeneous turbulence *Proc. R. Soc.* A **451** 87–104 (Osborne Reynolds Centenary Volume)

[13] Savill A M 1990 A synthesis of T3 test case predictions *Numerical Simulation of Unsteady Flows and Transition to Turbulence* ed O Pironneau *et al* (Cambridge: Cambridge University Press)

Savill A M 1996 *Turbulence and Transition Modelling* ed M Hallback *et al* (Dordrecht: Kluwer Academic) ch 6

[14] Schubauer G B and Klebanoff P S 1955 Contribution to the mechanism of boundary-layer transition *NACA T. N.* 3489

[15] Suzen Y B and Huang P G 2000 Modeling of flow transition using an intermittency transport equation *J. Fluids Eng.* **122** 273–84

[16] Tsuei H-S and Perot J B 2000 Turbomachinery predictions using the turbulent potential model *AIAA 2000–0135 (Reno, Nevada, January 2000)*

[17] Warsi Z U A 1999 *Fluid Dynamics Theoretical and Computational Approaches* (Boca Raton, FL: Chemical Rubber Company)
[18] Well C S 1967 Effects of free stream turbulence on boundary layer transition *AIAA J.* **5** 172–4
[19] White F M 1991 *Viscous Fluid Flow* (New York: McGraw-Hill)
[20] Van Driest E R and Blumer C B 1963 Boundary layer transition, free stream turbulence, and pressure gradient effects *AIAA J.* **1** 1303–6
[21] Zhang X and Perot J B 2000 Unsteady flow prediction of turbulent flow around a triangular cylinder *FEDSM 2000–11172 (Boston, MA, June 2000)*